Algal Research 71 (2023) 103024

Contents lists available at ScienceDirect

Algal Research

journal homepage: www.elsevier.com/locate/algal

The influence of physical floc properties on the separation of marine microalgae via alkaline flocculation followed by dissolved air flotation

N.R.H. Rao [a], A. Gonzalez-Torres [a], B. Tamburic [a,b], Y.W. Wong [a], I. Foubert [d,e], K. Muylaert [c], R.K. Henderson [a,*], D. Vandamme [a,c]

[a] AOM Lab, School of Chemical Engineering, The University of New South Wales, Sydney 2052, NSW, Australia
[b] Water Research Centre, School of Civil and Environmental Engineering, The University of New South Wales, Sydney 2052, NSW, Australia
[c] Laboratory for Aquatic Biology, KU Leuven Kulak, E. Sabbelaan 53, 8500 Kortrijk, Belgium
[d] KU Leuven Kulak, Research Unit Food & Lipids, Department of Molecular and Microbial Systems Kulak, Etienne Sabbelaan 53, B-8500 Kortrijk, Belgium
[e] Leuven Food Science and Nutrition Research Centre (LFoRCe), KU Leuven, Kasteelpark Arenberg 20, B-3001 Heverlee, Belgium

ARTICLE INFO

Keywords:
Biofuels
Biomass
Coagulation
Cyanobacteria
Ferric chloride
Nannochloropsis oculata
Water treatment

ABSTRACT

Flocculation achieved by raising the pH, termed alkaline flocculation is a sustainable way of inducing flocculation in marine microalgae. Flocs formed post-alkaline flocculation have the potential to be harvested via dissolved air flotation (DAF) or sedimentation. While DAF results in faster separation and biomass with a higher solids content compared to sedimentation, it has not been tested in saline environments, particularly when combined with alkaline flocculation. DAF processes, like most separation techniques, are heavily dependent on physical floc properties. In this study, the impact of alkaline floc properties on the performance of DAF versus sedimentation was evaluated to harvest marine *Nannochloropsis oculata*, benchmarking against the well-studied ferric chloride flocculation. This was followed by the use of the DAF *white-water* model to illustrate how alkaline and ferric floc properties impact bubble-particle attachment and DAF separation efficiencies. Alkaline flocs were smaller ($peak_{max}$ < 300 μm; majority flocs 130–470 μm), stronger (~70 % strength factor) and more compact (scattering exponent > 2.30) compared to ferric flocs which were larger ($peak_{max}$ ~ 1700 μm; >65 % of flocs >1000 μm), relatively weaker (<40 % strength factor), less compact (scattering exponent 1.49–2.30). However, as both flocs were hydrophilic, sedimentation yielded ~15 % greater efficiency than DAF. Stoke's Law suggested that sedimentation benefited due to alkaline floc compactness and large sizes of ferric flocs. Nonetheless, maximum separation efficiencies of ~80–85 % were still obtained via the DAF process. From the *white-water* model, bubble-floc attachment efficiency of alkaline flocs (0.01–0.001 %) was observed to be at least an order of magnitude greater than ferric flocs (0.001–0.0001 %) despite both methods resulting in comparable DAF separation efficiencies. For alkaline flocs, elevated bubble-floc attachment efficiency compensated low hydrophilicity; for ferric flocs, low bubble-floc attachment was compensated by large floc sizes. Overall, it is suggested that the determination of floc properties post-coagulation-flocculation could be used to optimise separation processes.

1. Introduction

The market demand for microalgal biomass is expected to increase in the coming years due to an increase in biomass use for energy and chemical production [1,2]. To increase microalgal biomass production while simultaneously reducing stresses on our limited freshwater resources, the use of marine microalgae such as *Nannochloropsis oculata* has been encouraged over terrestrial crops and freshwater microalgae. However, the small cell size (1–10 μm), low biomass concentration in the culture medium (~1 $g{\cdot}L^{-1}$), and high energy demands make separation of marine microalgae via conventional technologies, such as centrifugation or membrane filtration, energy-intensive and unsustainable [3,4]. Alternative methods are therefore necessary for the sustainable separation of marine microalgae from the culture medium.

The energy demand for separation can be reduced by aggregating individual cells into larger particles via flocculation [5–7]. Flocculation can be achieved in different ways, including: (a) dosing metal salts such as ferric chloride and alum, (b) dosing polymers, (c) increasing pH and

* Corresponding author at: School of Chemical Engineering, UNSW Sydney, Australia.
E-mail addresses: r.henderson@unsw.edu.au (R.K. Henderson), dries.vandamme@uhasselt.be (D. Vandamme).

https://doi.org/10.1016/j.algal.2023.103024
Received 27 November 2022; Received in revised form 7 February 2023; Accepted 13 February 2023
Available online 16 February 2023

allowing the existing magnesium ions in the culture medium to induce flocculation (alkaline flocculation), (d) using magnetic nanoparticles, and (e) induce bioflocculation due to algae-bacteria interactions [4,8–13]. Of these, alkaline flocculation by raising the pH is highly suitable as it is a simple, sustainable and inexpensive way of inducing flocculation in complex ionic systems such as saline water [4,14]. Nonetheless, further challenges arise during floc separation from within a saline medium.

Typically, the flocs are harvested from the culture medium by gravity sedimentation [6,15,16]. While sedimentation is cheap and consumes no energy, it is a relatively slow process resulting in the formation of a microalgal sludge with a high-water content [4,17,18]. It has been suggested that dissolved air flotation (DAF) could be used as an alternative to sedimentation. In DAF, a pressurised air-water mixture is introduced into the tank post-flocculation, after which air bubbles in the size range of 50–150 μm attach to flocs and rise to the top of the tank where the flocs can be skimmed off [3,5,6,19,20]. While the DAF process consumes energy during air-water pressurisation, it results in a faster separation and a biomass with a higher solid-liquid ratio compared to sedimentation, thereby decreasing downstream processing costs [3,5,19]. However, unlike sedimentation, DAF application in saline environments is complex and presents challenges due to the high salt concentrations present. For instance, the air solubility and air transfer efficiency are lower in saline water compared to freshwater, and thus, the recycle ratio and saturator pressure for separating marine microalgae need to be higher to provide equivalent conditions to those used for freshwater microalgae [21–23]. While both, sedimentation and DAF processes have relative advantages and limitations, there is a lack of research on DAF usage for separating marine microalgae, particularly post-alkaline flocculation. Hence, it is unclear if DAF is a suitable separation option for this application.

DAF processes, like most separation techniques, are heavily dependent on the physical floc properties [15,24,25]. Generally, sedimentation is favoured by large and compact flocs with fast settling rates; in contrast, DAF is typically more suited to less compact, hydrophobic, pinpoint (small) flocs that are known to improve adherence to bubbles, maximise rise velocity and minimise floc rupture caused by turbulence created upon bubble injection [24,26,27]. While previous studies that evaluated marine microalgal floc properties examined metal-salt based flocculation (ferric, titanium chloride) and polymeric flocculation, the analysis of alkaline floc properties of marine microalgae has been constrained to floc size only [28–31]. Other physical floc properties such as strength, compactness, and hydrophobicity-hydrophilicity, which can influence separation performance have not been investigated and thus, their impact on alkaline floc separation via sedimentation and DAF processes is currently unknown.

Unlike gravity sedimentation, DAF operation is complex and in addition to the physical floc properties, the DAF separation efficiency can be influenced by the DAF operating parameters [24]. This has been demonstrated in detail through the development of the empirical *white-water* DAF model (SI Eq. S1, refer SI Section S1 for full details on the model) [24,25,32]. The model treats DAF operation as a blanket of bubbles that behave as collectors of particles. As a result, parameters that influence effective bubble-particle interaction and attachment including floc size, bubble size, bubble concentrations and bubble rise velocities can influence DAF separation outcomes [24]. Of these, the bubble concentrations and rise velocities are further influenced by the recycle ratio which is a percentage of the clarified water that is recycled back into the saturator to generate microbubbles, and the DAF saturator pressure [24,32]. Therefore, a systematic evaluation each of the aforementioned parameters is required to understand their influence on DAF separation outcomes.

Thus, the main innovations of this study were threefold: (a) to evaluate the performance of the DAF process to harvest the alkaline flocs of the marine microalgal species *Nannochloropsis oculata* and benchmark this performance against conventional ferric chloride-based flocculation method and the sedimentation process; (b) to examine in detail a range of physical properties including size, strength, compactness, and hydrophobicity/hydrophilicity of alkaline flocs and assess separation performance in the context of the differing floc properties in marine medium; (c) to illustrate the impact of differing floc sizes and DAF process parameters on bubble-particle attachment and DAF separation efficiency via the *white-water* model.

2. Materials and methods

2.1. Cultivation of Nannochloropsis oculata in an outdoor raceway pond using artificial seawater

Nannochloropsis oculata CS-179 was obtained from the Commonwealth Scientific and Industrial Research Organisation's (CSIRO) Australian National Algae Culture Collection (ANACC), Hobart, Australia. The culture was inoculated in a 500 L outdoor aerated raceway pond using artificial seawater (salinity: 32 $g{\cdot}L^{-1}$) enriched with f/2 medium [12]. The culture was maintained in turbidostatic conditions at a biomass concentration of 1 $g{\cdot}L^{-1}$ for 3 weeks. During this period, samples were taken to perform all described experiments.

2.2. Evaluation of sedimentation versus DAF for separating Nannochloropsis oculata

2.2.1. Jar testing

Bench scale flocculation, sedimentation and DAF jar tests were conducted using a Platypus Jar Tester (Aquagenics Pty Ltd., Australia) which had 76 × 25 mm flat paddle impellers and 1 L square jars. Ferric chloride powder (97 %) and sodium hydroxide pellets (97 %) were obtained from Sigma-Aldrich (Australia) and used for flocculation experiments. 1 M hydrochloric acid and sodium hydroxide solutions were used to control the pH during jar testing. Microalgal suspensions of 2 L at a biomass concentration of 1 $g{\cdot}L^{-1}$ were evaluated in four types of jar tests as follows:

- Test 1: Ferric chloride flocculation-sedimentation
- Test 2: Alkaline flocculation-sedimentation
- Test 3: Ferric chloride flocculation-DAF
- Test 4: Alkaline flocculation-DAF

Flocculation was conducted based on previously published protocols [27,33–35]. Briefly, microalgal suspensions were initially stirred at 200 rpm for 2 min. During this time: (a) for tests 1 and 3, ferric chloride was dosed at various concentrations between 0 and 10 $mg{\cdot}L^{-1}$ followed by pH adjustment to 7, and (b) for tests 2 and 4, sodium hydroxide was dosed at various concentrations between 0 and 250 $mg{\cdot}L^{-1}$. The pH was continuously monitored. A slow stirring phase at 30 rpm for 30 min to promote floc growth was then followed in all tests. The difference in the dose ranges of ferric chloride (0–10 $mg{\cdot}L^{-1}$) and sodium hydroxide (0–250 $mg{\cdot}L^{-1}$) is due to the differing floc formation mechanisms. Generally, sweep flocculation tends to be predominant at high doses and high pH, for example, at >50 $mg{\cdot}L^{-1}$ of sodium hydroxide [35]; charge neutralisation tends to be predominant at relatively low doses and/or slightly acidic pH value, for example, <5 $mg{\cdot}L^{-1}$ of ferric chloride [36]; and a combination of charge neutralisation and sweep flocculation tend to be influential when increasing the dose of ferric chloride, for example, at 10 $mg{\cdot}L^{-1}$ [4].

Sedimentation: In tests 1 and 2, following slow stirring, a 30 min settling period with no stirring was implemented to allow floc sedimentation [27,33].

DAF: In tests 3–4, an air-artificial seawater mixture (salinity controlled at 32 $g{\cdot}L^{-1}$) was pressurised to 500 kPa in the saturator and released into the jar immediately after flocculation. Flotation was conducted for 10 min with a recycle ratio of 20 % [5,23].

2.2.2. Analysis of sedimentation and dissolved air flotation performance

The analysis undertaken to assess and lend insight into sedimentation and DAF performance included: (a) zeta potential measurements of the clarified water using a Zetasizer Nano ZS (Malvern, Australia), and (b) evaluation of the sedimentation and DAF separation efficiencies and concentration factors. The sedimentation and DAF separation efficiencies were determined by measuring the sample absorbance at 750 nm, which is commonly described as the optical density (OD), before flocculation (OD_i) and after sedimentation or DAF (OD_f) (Eq. (1)) [29].

$$\text{Separation efficiency} = \frac{OD_i - OD_f}{OD_i} \times 100 \quad (1)$$

The concentration factor was determined by dividing the total volume (2000 mL) by the volume of the particulate phase after separation [37].

2.3. Floc property analysis

The hydrophilicity of flocs was analysed via contact angle measurements in a fully automated optical tensiometer (Theta ATA Scientific, Australia) [38,39]. Alkaline (180 mg·L^{-1}) and ferric flocs (3 mg·L^{-1}) were collected after separation, placed on a glass slide and dried for 2 h at 50 °C. The contact angle was measured post-addition of 500 μL of artificial seawater medium on each floc-glass slide; comparisons were made to a glass slide with only the 500 μL artificial seawater medium (control). The average contact angle measured after 10 s for triplicate experiments was reported.

To evaluate the influence of floc properties on sedimentation and DAF performance, two concentrations of sodium hydroxide and ferric chloride corresponding to moderate (~70–75 %) and high (>90 %) cell separation were chosen from each of Tests 1–4 and used to generate flocs. The following floc properties were then analysed using a Mastersizer 3000 (Malvern, Australia) based on previously published procedures [33,40,41]: growth rate, size, strength and recovery factors, and compactness. Briefly, the results of the median average equivalent diameter (d_{50}) of the flocs were used to generate the floc growth curve, which was then used to determine the floc growth rate. Subsequently, the average of all steady-state floc sizes from 4 to 24 min (at 30 rpm; growth period), 24–42 min (at 200 rpm; breakage period), and 42–57 min (at 30 rpm; regrowth period) were evaluated. Floc strength factor was calculated based on the floc size before breakage (24 min) and after breakage (32 min). Recovery factor was calculated based on the floc size before breakage (24 min), after breakage (32 min) and during the regrowth period (50 min). Scattering exponents, which indicate degree of floc compaction, were calculated at different time points from 10 to 50 min. Values of the scattering exponent vary between 1 and 3, where the closer the value is to 3 the higher the degree of compaction that is expected. Floc properties for the different flocculation methods were statistically compared using a one-way analysis of variance (ANOVA) with a level of significance set at 0.05 using Microsoft Excel 2019.

2.4. Lending insight into experimentally obtained dissolved air flotation separation efficiencies using the white-water model

Insight into the experimentally obtained DAF separation efficiencies when using alkaline and ferric chloride flocculation methods were obtained via the empirical *white-water* DAF model performance equation described in detail by Haarhoff and Edzwald [25].

$$\left(1 - \frac{n_{p,e}}{n_{p,i}}\right) = \left\{1 - exp\left(\frac{\frac{-3}{2}\alpha_{pb}\eta_T\varphi_b\nu_b t_{cz}}{d_b}\right)\right\} \quad (2)$$

where $\left(1 - \frac{n_{p,e}}{n_{p,i}}\right)$ = DAF separation efficiency (dimensionless); $n_{p,e}$ and $n_{p,i}$ = concentration of particles in the treated and influent water (particles·mL^{-1}), respectively; α_{pb} = attachment efficiency (dimensionless); η_T = particle transport coefficient (dimensionless); ϕ_b = bubble volume concentration (m^3 air · 10^{-6} m^{-3} water); ν_b = bubble rise velocity (m·s^{-1}); t_{cz} = microbubble residence time in the DAF contact zone (s); d_b = bubble diameter (m); Refer SI Section S1 for complete details on how the different parameters were obtained or calculated.

2.4.1. Impact of differing floc size on DAF separation efficiency

The *white-water* model uses a single average particle size (d_p) to model the DAF separation efficiency (SI Section S1). However, in reality, flocs of varying sizes and volume densities can form during microalgal flocculation. Biases and discrepancies between the experimentally obtained and modelled efficiencies can occur if the varying floc sizes are not accounted for in the *white-water* model. Thus, the model was used to predict the contribution of different floc size categories (measured as described in Section 2.3) to the experimentally obtained DAF separation efficiency. Five attachment efficiencies of 1, 0.1, 0.01, 0.001, 0.0001 were evaluated. The measured floc sizes and their measured concentration (vol%) for each flocculation method was matched with their predicted DAF separation efficiency. The relative contribution of each floc size category to the relative DAF separation efficiency was then calculated as a function of the differing attachment efficiencies. Refer SI Section S2 for detailed procedure.

2.4.2. Impact of differing bubble size, saturator pressure and recycle ratio on DAF separation efficiency

The *white-water* model uses a single average bubble size (d_b) to model the DAF separation efficiency (SI Section S1). However, DAF microbubble sizes range from 50 to 150 μm and bubbles of different sizes have different particle transport coefficients (Eqs. S2-S5, SI Section S1.1) and rise velocities (Eq. S10, SI Section S1.3). Thus, the contribution of different floc size categories to the experimentally obtained DAF separation efficiency were evaluated at different attachment efficiencies for bubble sizes of 50 μm, 100 μm, 150 μm. Values for saturator pressure and recycle ratio were set at 500 kPa and 20 %, respectively.

The air solubility and air transfer efficiency are lower in saline water compared to freshwater, and thus, the recycle ratio and saturator pressure used in seawater DAF operation are usually higher than that used for freshwater DAF. Varying the saturator pressure and recycle ratio can influence the bubble volume concentration (Eqs. S6-S9, SI Section S1.2). Therefore, the model was used to predict the contribution of different floc size categories to the experimentally obtained DAF separation efficiency at different attachment efficiencies when: (a) varying saturator pressures from 400 to 600 kPa at 20 % recycle ratio, and (b) 10 % and 15 % recycle ratio at 500 kPa saturator pressure. The bubble size was kept constant at 85 μm based on previous measurement [42].

3. Results

3.1. Separation efficiency of Nannochloropsis oculata by DAF and sedimentation using ferric chloride and alkaline flocculation

The use of DAF or sedimentation as the separation process and the flocculation method applied influenced *N. oculata* separation outcomes (Fig. 1). Sedimentation resulted in ~10–15 % higher efficiencies than DAF for both flocculation methods with increasing coagulant dose (p-value <0.05) (Fig. 1 A-B). These results contrast established literature, which usually suggests that DAF achieves better algal separation efficiencies than sedimentation due to the natural buoyancy of microalgal cells [24,44], and is explored further in Section 3.3.

Ferric chloride flocculation resulted in median separation efficiencies of ~77 % (DAF) and 100 % (sedimentation) at 5 mg·L^{-1} ferric chloride dose (Fig. 1 A-B). This marginally improved to ~80 % (DAF) and remained stable at 100 % for sedimentation as the ferric chloride dose was increased to 10 mg·L^{-1} (Fig. 1 A-B). Alkaline flocculation resulted in maximum separation efficiencies of ~85 % (DAF) and 100 %

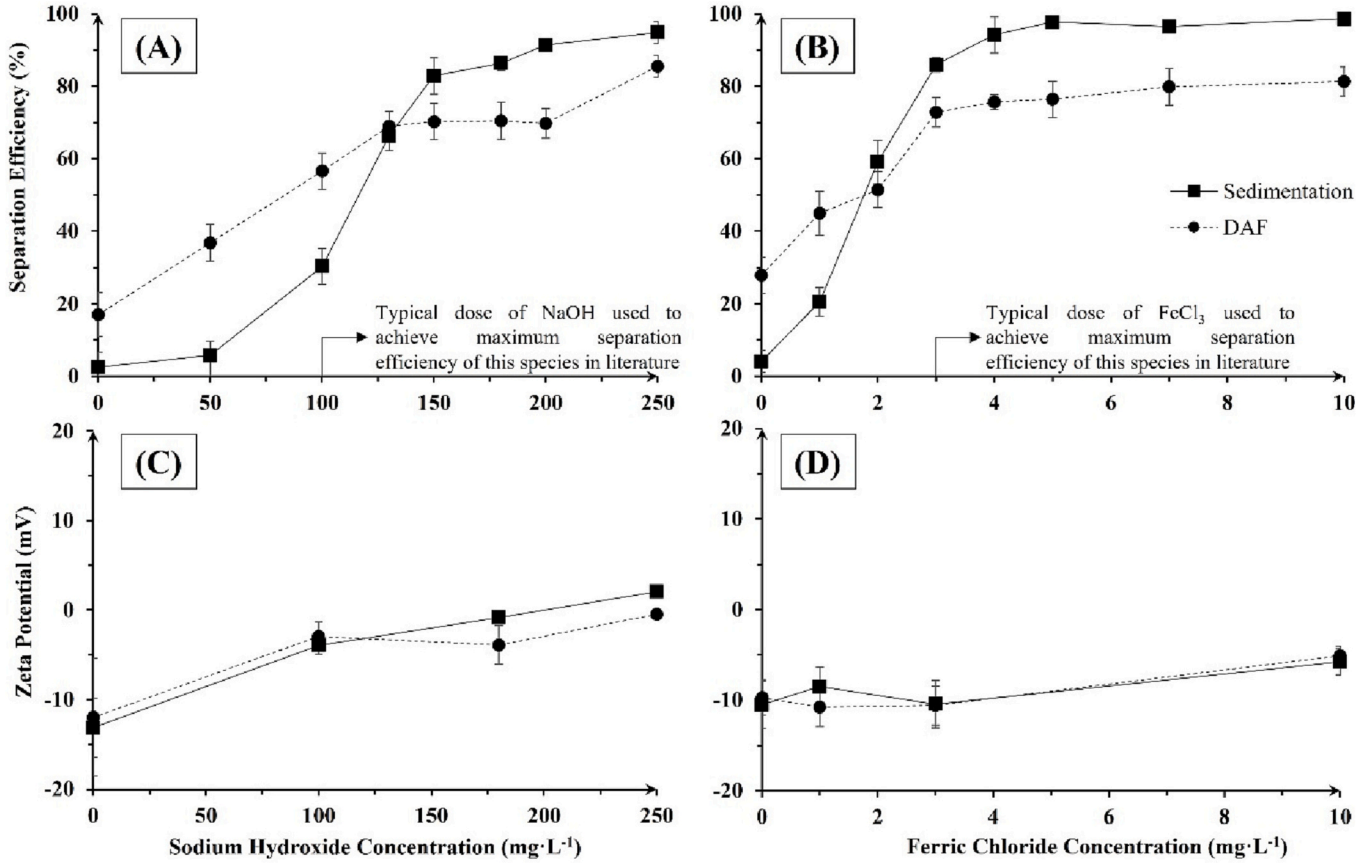

Fig. 1. Separating *Nannochloropsis oculata* cells via DAF and sedimentation using alkaline (A, C, E) and ferric chloride (B, D, F) flocculation; A-B: separation efficiency; C-D: zeta potential, as functions of chemical dose. Typical dose required for achieving maximum separation efficiency for this species via sedimentation – 100 mg·L^{-1} sodium hydroxide [29,43]; 3 mg·L^{-1} ferric chloride [29].

(sedimentation) only at the highest dose trialled – 250 mg·L^{-1} (Fig. 1 A-B), which was significantly higher than the sodium hydroxide dose of 100 mg·L^{-1} used previously to obtain maximum separation efficiencies of >95 % for the same species [29,43]. This was because the microalgal concentration used in the current study was 2.5–3.3× higher (1 g·L^{-1}) than the microalgal concentration of 0.30–0.40 g·L^{-1} used in those studies [29,43]. The cell concentration is known to affect the dose of the flocculant; this is because as the cell concentration increases, a greater dose of the flocculant is required to neutralise the negatively charged cells and aggregate them into flocs [45]. Therefore, in the current study,

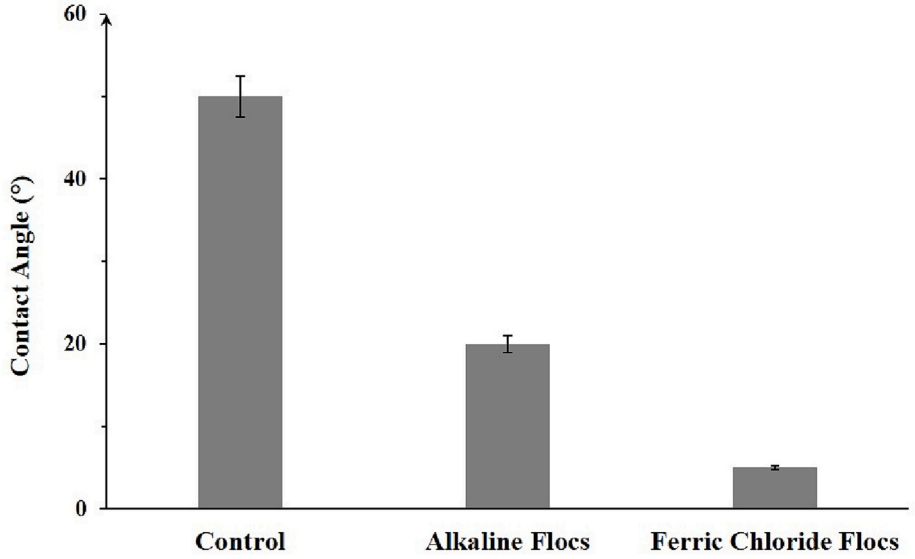

Fig. 2. Contact angle of *Nannochloropsis oculata* flocs measured prior to separation via DAF or sedimentation. Flocs were generated via low dose (180 mg·L^{-1}) sodium hydroxide and low dose (3 mg·L^{-1}) ferric chloride (p-value = 3.2 × 10^{-6}). Contact angle measurements were used as a surrogate for hydrophilicity analysis; lower contact angle is representative of higher hydrophilicity.

the dose of sodium hydroxide used to obtain maximum separation was greater than the 100 mg·L^{-1} used in previous studies [29,43].

The magnitude of the zeta potential of clarified water became less negative, approaching 0 mV with increasing dose of sodium hydroxide and ferric chloride (−11.3 ± 2.2 mV to +0.9 ± 3.6 mV for alkaline and −11.3 ± 2.2 mV to −3.9 ± 2.1 mV for ferric chloride) (Fig. 1 C-D), supporting the increasing efficiency of both coagulants with dose [33,46]. Interestingly, while enhanced sedimentation and DAF efficiencies were observed at high coagulant doses, positive effluent zeta potentials were not observed (Fig. 1 C-D). This was most likely due to the compression of the electrical double layer around the particle, commonly observed in saline environments [36].

3.2. Characterisation of alkaline and ferric floc properties

3.2.1. Hydrophobic/hydrophilic characteristics of flocs

Evaluation of the hydrophobic/hydrophilic nature of flocs via contact angle measurements revealed that both types of flocs were hydrophilic (Fig. 2), with the ferric flocs more hydrophilic than the alkaline flocs (p-value = 3.2 × 10^{-6}) (Fig. 2). The general hydrophilicity of the alkaline and ferric flocs might explain the lower separation efficiency via DAF when compared to sedimentation (Fig. 1 A-B); as previously mentioned, DAF bubbles are hydrophobic and thus interact with flocs via hydrophobic interactions [24,26]. Despite the greater hydrophilicity of the ferric flocs, the observed DAF separation efficiencies for alkaline and ferric flocs were statistically similar at low dose (DAF separation: ~70 %; alkaline: 180 mg·L^{-1}; ferric: 3 mg·L^{-1}) and statistically similar at high dose (DAF separation: ~80–85 %; alkaline: 250 mg·L^{-1}; ferric: 10 mg·L^{-1}) (p-value >0.05) (Fig. 1 A-B). Hence, additional floc characteristics including size, strength and compaction and the bubble-floc attachment efficiencies were explored.

3.2.2. Floc properties in the floc growth period

Significant differences were observed in the floc size and volume densities between alkaline and ferric flocs measured in the growth period. In general, the alkaline flocs at both doses of sodium hydroxide had smaller steady-state floc sizes (270–293 μm) than the ferric flocs (low dose: 749–945 μm; high dose: 1498–1564 μm) (p-value = 0.001) (Table 1), which can be attributed to the differing mechanisms behind floc formation between the flocculation methodologies [29]. Further analysis (at 24 min) showed that the alkaline flocs had a broad monomodal distribution with a size range of 12–2000 μm and a peak maximum at 277–286 μm irrespective of the concentrations (p-value = 0.47, Table S3) (Fig. 3). In contrast, the ferric flocs had a multi-modal distribution that was dose-dependent (p-value <0.05, Table S3); for instance, the low dose ferric flocs resulted in several peaks ranging from 1 to 4 μm ($Peak_{max}$ = 1.8 μm, likely to be free cells), 10–78 μm ($Peak_{max}$ = 33 μm), 80–392 μm ($Peak_{max}$ = 168 μm), 625–2000 μm ($Peak_{max}$ = 1672 μm), whereas the high dose ferric flocs resulted in two peaks ranging from 103 to 388 μm ($Peak_{max}$ = 192 μm) and 385–2000 μm ($Peak_{max}$ = 1583 μm) (Fig. 3). In terms of the volume densities of the different size distributions, >50 % of the low and >65 % high dose ferric flocs were > 1000 μm in size, compared to the low and high dose alkaline flocs which were smaller and where the majority ranged from 130 to 470 μm (Fig. 3). These results suggest that floc size can be impacted by the differing floc formation mechanisms.

In addition to smaller sizes, the alkaline flocs grew at a steady pace (280–343 μm·min^{-1}) and were compact (2.37–2.41) irrespective of whether low or high concentrations of sodium hydroxide were dosed (p-value >0.05, Tables S3-S4) (Tables 1, 2, Fig. 4). In comparison, the properties of the ferric flocs fluctuated with the ferric chloride concentrations; low dose ferric flocs grew slowly (48 ± 18 μm·min^{-1}) and had low compaction (1.41–1.85) compared to the high dose ferric flocs which produced the fastest growing flocs (485 ± 112 μm·min^{-1}) with good compaction (2.19–2.29) (p-value <0.05, Tables S3-S4) (Tables 1, 2, Fig. 4). Advanced floc property data for alkaline flocs, particularly in saline environments is limited in the literature. Yet, the results fit the trends observed in previous studies which suggest that sweep flocculation leads to a greater floc compaction due to the tight enmeshment of hydroxide precipitates and particles, than flocs formed via charge neutralisation [36,40,47].

3.2.3. Floc properties in the floc breakage period

In the floc breakage period, 33 %, 85 % and 67 % declines in the steady-state floc sizes were observed for the alkaline, low dose ferric and high dose ferric flocs, respectively, resulting in high (66–71 %), low (10–16 %) and low-medium (30–40 %) strength factors for the same three floc types (p-values for floc size upon breakage and strength factor < 0.05) (Table 1, Fig. 4). While data on floc properties post-breakage for alkaline flocs is scarce, it is well known that during high pH (>10) alkaline flocculation, microalgal cell walls become rigid and do not get deformed easily due to the lack of bioavailable carbon, thereby resulting in negligible diffusion across the cell wall [12,48]; this likely contributed to the enhanced floc strength. In the case of ferric flocs, similar floc strengths and significant decreases in floc sizes upon breakage have been observed in freshwater *Chlorella vulgaris* and *Microcystis aeruginosa*, and marine *Chlorella vulgaris* and *Chaetoceros muelleri*, and has been previously attributed to floc formation via the charge neutralisation mechanism [27,33,49,50]. Interestingly, floc-compactness before and after breakage remained stable for the alkaline flocs (p-value >0.05, Table S4) and high dose ferric flocs (p-value >0.05, data not shown), whereas it increased significantly from 1.41 to 1.65 (before breakage) to 1.98–2.49 (after breakage) for the low dose ferric flocs (p-value >0.05, data not shown) (Table 2). This could indicate that the low dose ferric flocs were formed via smaller clusters of compact flocs.

Collectively, the floc properties post-breakage suggest that the: (a) small-sized alkaline flocs which had high strength and compaction resisted breakage and eroded into small (<10 μm) particles; (b) large-sized low dose ferric flocs which had low strength and compaction underwent breakage via fragmentation to form highly compact particles; and (c) large-sized high dose ferric flocs which had low-medium strength but high compaction underwent breakage via both fragmentation and erosion. This breakage mechanism is supported by the minimal (10–15 %), moderate (20–45 %) and substantial (50–90 %; includes formation of new peaks) changes observed in the volume densities of the different size distribution peaks and the floc sizes of the alkaline, low

Table 1
Properties of *Nannochloropsis oculata* flocs obtained during alkaline and ferric chloride flocculation.

Flocculation method	Dose	Floc growth rate	Steady-state floc size			Strength factor	Recovery factor
			Growth	Breakage	Regrowth		
	(mg·L^{-1})	(μm·min^{-1})	(μm)	(μm)	(μm)	(%)	(%)
Alkaline	180	314 ± 34	279 ± 9	189 ± 1	187 ± 0.4	68 ± 2	-3 ± 0.4
	250	325 ± 18	281 ± 12	197 ± 11	190 ± 5	70 ± 1	-9 ± 8
Ferric chloride	3	48 ± 18	847 ± 98	113 ± 19	628 ± 178	13 ± 3	69 ± 6
	10	485 ± 112	1531 ± 33	572 ± 111	757 ± 17	35 ± 5	19 ± 3
p-Value		0.001	1.2 × 10^{-5}	7.2 × 10^{-4}	0.001	3.7 × 10^{-5}	7.3 × 10^{-5}

p-Values determined using one-way ANOVA with α = 0.05.

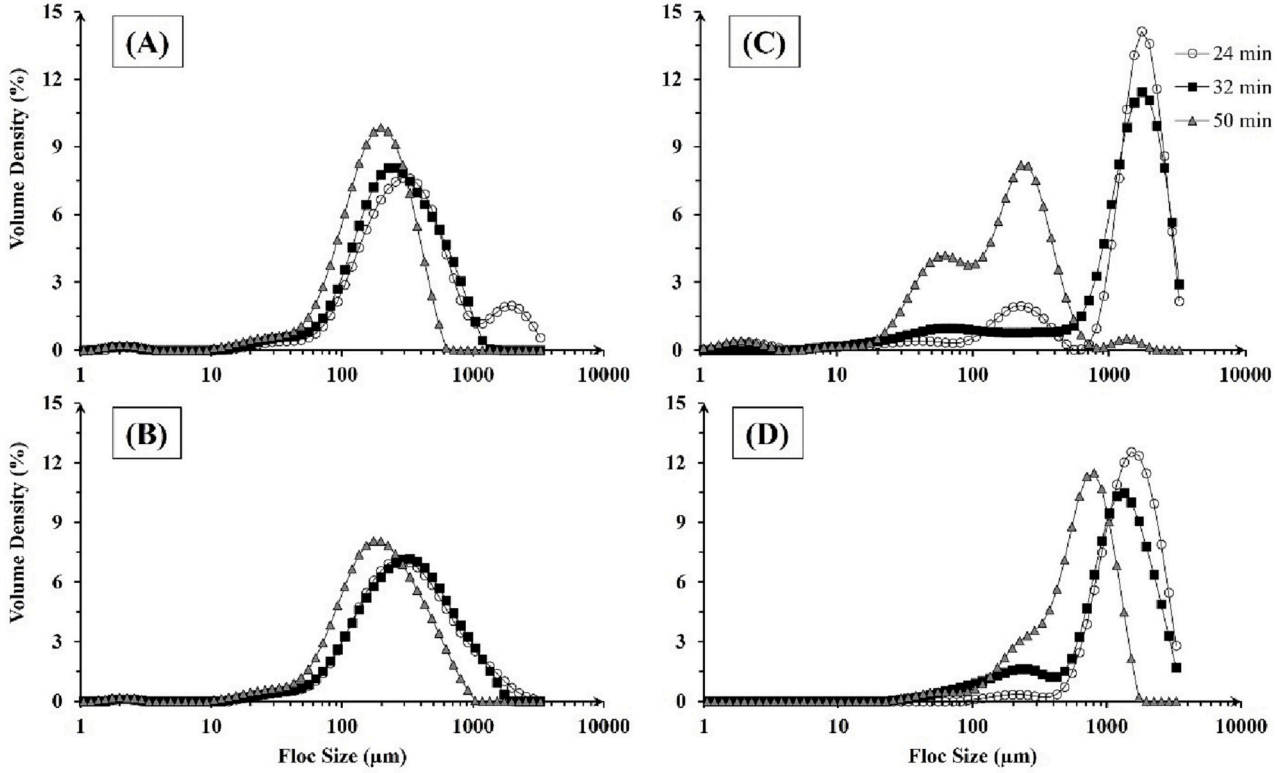

Fig. 3. Floc size and volume distribution at various time points in growth (24 min), breakage (32 min) and regrowth (50 min) periods of flocs for alkaline flocculation using (A) 180 mg·L^{-1} and (B) 250 mg·L^{-1} of sodium hydroxide, and for ferric chloride flocculation using (C) 3 mg·L^{-1} and (D) 10 mg·L^{-1} of ferric chloride.

Table 2
Scattering exponents of *Nannochloropsis oculata* flocs obtained during alkaline and ferric chloride flocculation. Scattering exponents vary from 1 to 3 and compactness increases as scattering exponent increases.

Flocculation method	Dose (mg·L^{-1})	Scattering exponent					
		Before floc breakage		After floc breakage			After floc regrowth
		10 min	20 min	30 min	35 min	40 min	50 min
Alkaline	180	2.39 ± 0.02	2.37 ± 0.03	2.35 ± 0.00	2.34 ± 0.00	2.32 ± 0.03	2.37 ± 0.02
	250	2.40 ± 0.01	2.40 ± 0.01	2.37 ± 0.02	2.37 ± 0.02	2.33 ± 0.01	2.37 ± 0.02
Ferric chloride	3	1.61 ± 0.04	1.53 ± 0.12	1.99 ± 0.01	2.21 ± 0.00	2.39 ± 0.10	2.21 ± 0.03
	10	2.24 ± 0.04	2.24 ± 0.05	2.22 ± 0.04	2.26 ± 0.16	2.23 ± 0.20	2.29 ± 0.14
p-Value		2.8×10^{-9}	5.6×10^{-7}	1.2×10^{-7}	0.13	0.43	0.078

p-Values determined using one-way ANOVA with $\alpha = 0.05$.

dose ferric, and high dose ferric flocs, respectively (Tables 1, 2, Figs. 3–4).

3.2.4. Floc properties in the floc regrowth period

Fragments of ferric floc demonstrated the ability to regrow after floc breakage, as indicated by positive recovery factors, increasing floc size and volume density of particles during the regrowth period (Table 1, Figs. 3–4). Among the ferric flocs, the low dose ferric flocs had a higher recovery factor, resulting in these flocs growing back to 65–75 % of their size prior to the floc breakage, unlike the high dose ferric flocs which only regrew to ~20 % of their size prior to floc breakage (Table 1, Fig. 4). In contrast to the ferric flocs, floc regrowth was completely absent in the alkaline flocs at both sodium hydroxide doses (p-value <0.05) (Table 1, Figs. 3–4). It has been previously demonstrated that flocs of marine *C. vulgaris* and freshwater *M. aeruginosa* formed by sweep flocculation had a reduced recovery rate compared to those formed through charge neutralisation, which was attributed to sweep flocs having covalent chemical bonds (e.g. hydroxides of metal-salt precipitates with carboxyl and phenol groups of organic molecules) which undergo irreversible damage during breakage [27,33,50]. The observations in the current study are thus supported by the literature and suggest that floc fragmentation was more conducive to floc regrowth due to the instigation of physical bonding between particles via electrostatic, Van der Waals and other structural forces, while the erosion of flocs into smaller particles inhibited floc regrowth.

The floc compactness for the low and high dose alkaline and ferric flocs during the floc breakage and regrowth periods were comparable (p-values >0.05, data not shown) (Table 2). This observation was particularly interesting in the case of ferric flocs because it implied that the high dose ferric flocs regrew into larger flocs with similar compaction that was observed before floc breakage (Table 2). In contrast, the low dose ferric flocs regrew into larger flocs with greater compaction than what was achieved before floc breakage (Table 2). Overall, this suggests that fragmented flocs can regrow into more compact flocs during the regrowth period.

3.3. Impact of differing floc sizes on bubble-floc attachment and DAF separation efficiency: insights from DAF modelling

The DAF separation efficiency as a function of varying attachment

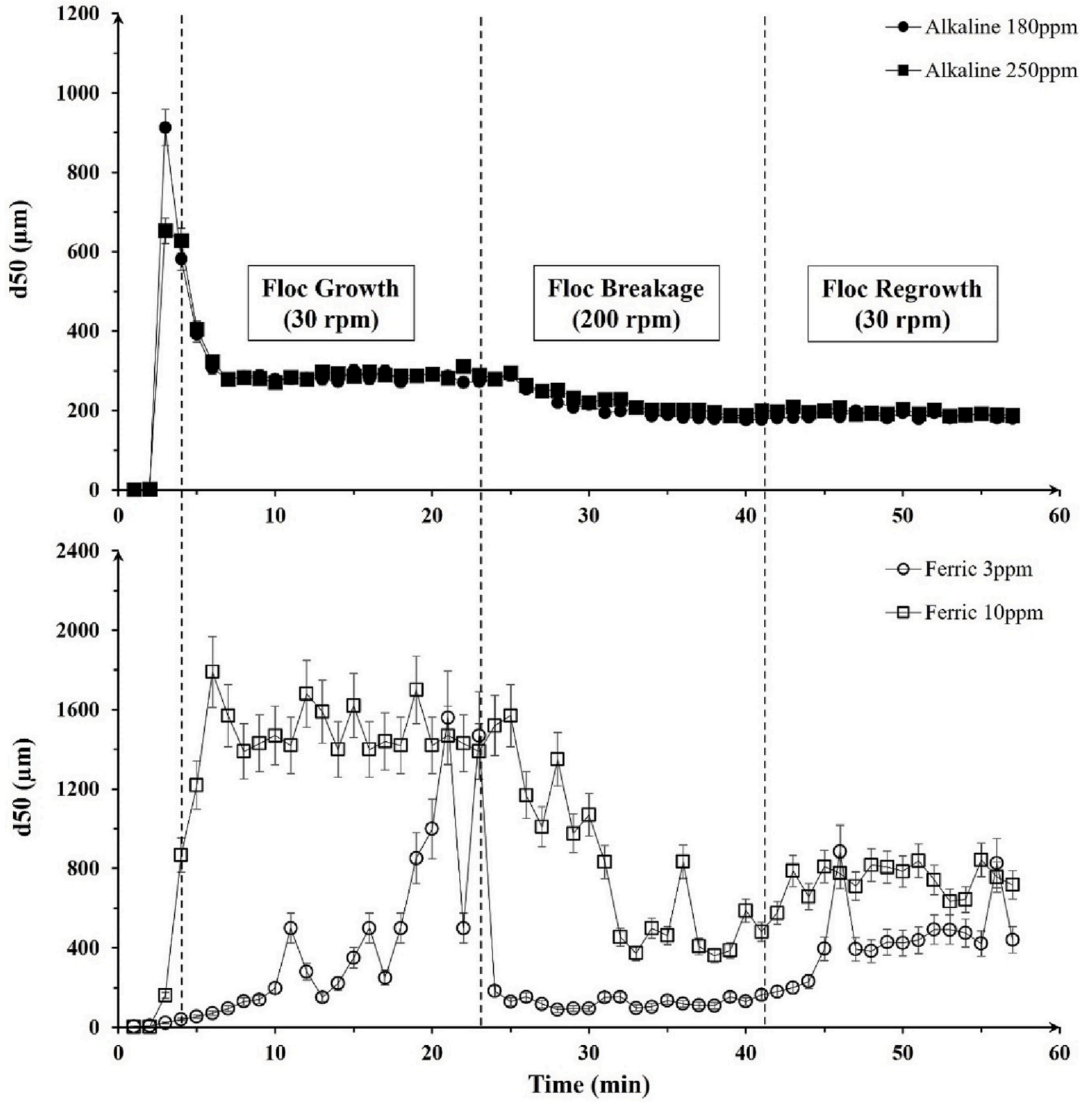

Fig. 4. Floc size (d_{50}) analysis of *Nannochloropsis oculata* during floc growth, breakage and regrowth over time. Alkaline flocs generated using low dose (180 mg·L^{-1}) and high dose (250 mg·L^{-1}) of sodium hydroxide, respectively; ferric flocs generated using low dose (3 mg·L^{-1}) high dose (10 mg·L^{-1}) of ferric chloride, respectively.

efficiencies was initially modelled for each experimentally obtained floc size range using the empirical DAF *white-water* model (Table S2). As expected, the modelled separation efficiency increased with the attachment efficiency for both doses of alkaline and ferric flocs (Table S2). Comparisons between the modelled and experimentally obtained DAF separation efficiencies revealed that the most probable attachment efficiencies for the alkaline flocs (low dose: between 0.01 and 0.001; high dose: ~0.01) were at least an order of magnitude greater than those of the ferric flocs (low dose: between 0.001 and 0.0001; high dose: ~0.0001) (Table S2). Furthermore, only the alkaline flocs followed the model prediction – increasing DAF separation efficiency with increasing attachment efficiency (Table S2). In contrast to model prediction, the experimentally obtained DAF separation efficiency for the high dose ferric flocs was higher at a lower attachment efficiency and vice versa (Table S2). Such observations can be attributed to variations in DAF operating parameters and floc size [42,51,52].

In this study, no significant differences were observed when varying the DAF operating parameters – bubble size (between 50 and 150 µm), saturator pressure (between 400 and 600 kPa), and recycle ratio (between 10 and 20 %) (Figs. S2-S4). However, when the floc size contributions were analysed, it was observed that irrespective of the dose concentrations and at the probable attachment efficiencies (previous paragraph, Table S2), alkaline flocs between 101 and 500 µm and ferric flocs >1000 µm mainly contributed to the experimentally obtained DAF separation efficiencies (red highlights in Fig. 5). This suggests that greater floc sizes can compensate for low bubble-floc attachment efficiencies as was observed in ferric flocs. Overall, out of the variable *white-water* model parameters: floc size, bubble size, saturator pressure and recycle ratio, the floc size (experimentally obtained) had the most impact on DAF separation.

4. Discussion

4.1. Linking floc properties to sedimentation and DAF separation efficiencies

In this study, the alkaline flocs of *N. oculata* generated by sodium hydroxide dosing were found to be less hydrophilic, smaller, stronger and more compact compared to the ferric flocs that were more hydrophilic, larger, relatively weaker and less compact (dose-dependent) (Fig. 3, Tables 1, 2). Established knowledge suggests that DAF is typically suited to less hydrophilic, stronger and smaller flocs unlike sedimentation that favours large flocs; settling rates are proportional to square of particle size according to Stoke's Law [24,26,27]. However, an

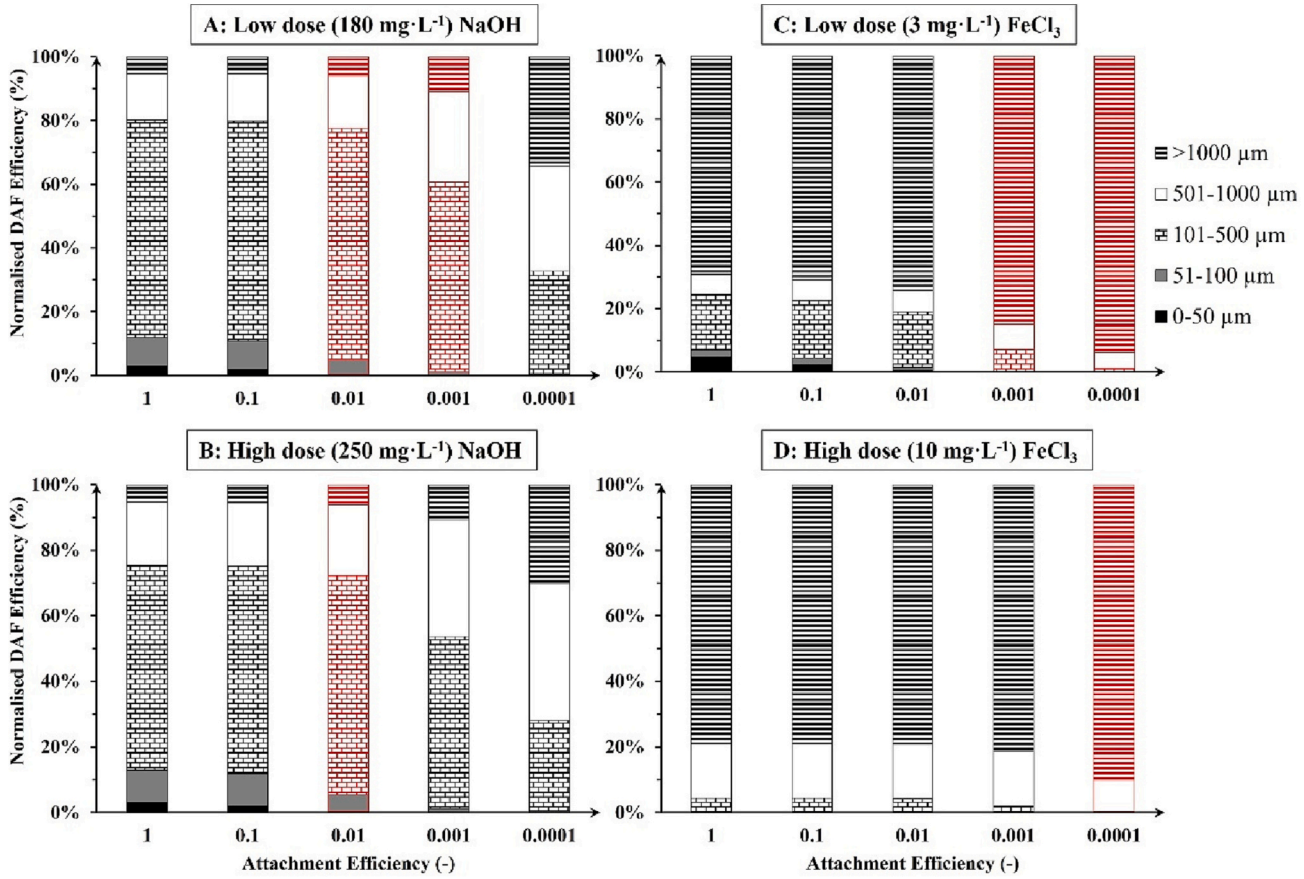

Fig. 5. Relative contribution of different *Nannochloropsis oculata* floc sizes (d_{50}) to bubble-floc attachment and modelled dissolved air flotation separation efficiencies (normalised to 100 %) calculated using the *white-water* model. Alkaline flocs generated using (A-B) low (180 mg·L^{-1}) and high (250 mg·L^{-1}) dose of sodium hydroxide, respectively; ferric flocs generated using (C-D) low (3 mg·L^{-1}) and high (10 mg·L^{-1}) dose of ferric chloride, respectively. Red highlights indicate the most likely attachment efficiencies at the experimentally obtained DAF separation efficiencies. Please refer to SI Section S2 for the full procedure on how the data was obtained. (For interpretation of the references to colour in this figure legend, the reader is referred to the web version of this article.)

analysis of the results showed that the maximum separation efficiency of *N. oculata* was ~10–15 % higher ($p < 0.05$) at the optimum dose for sedimentation (~100 %) than for DAF (80–85 %) during both alkaline and ferric chloride flocculation (Fig. 1). This implies that depending on the flocculation methodologies applied, some floc properties can be more influential than others when determining the choice of the separation process.

In the case of sedimentation, it is proposed that the high degree of compactness of the alkaline flocs compensated for their comparatively smaller floc sizes (with ferric flocs) and was beneficial in improving the *N. oculata* floc sedimentation efficiency; according to Stoke's Law, sedimentation rate can be improved by increasing the compactness of the particle [53]. Similar observations have been made for alum-based *Chlorella vulgaris* flocs where relatively compact flocs (scattering exponent ~ 1.9) with sizes <300 µm settled faster than less compact flocs (scattering exponent < 1.5) with sizes >300 µm [54]. This implies that floc compactness plays a major role in determining sedimentation outcomes for the alkaline flocs.

While not as effective as sedimentation, the DAF process still resulted in maximum separation efficiencies of ~80–85 % for both types of flocs (Fig. 1). Analysis of the *white-water* model revealed that the DAF separation efficiencies were mostly driven by flocs >1000 µm in size for ferric chloride flocculation and flocs between 101 and 500 µm in size for the alkaline flocculation method (Fig. 5). The large-sized (>1000 µm) ferric flocs in particular were able to overcome low bubble-floc attachment efficiencies and achieved maximum separation efficiencies of ~80–85 %. Furthermore, ferric flocs possessed the ability to regrow into relatively large flocs post-floc breakage (Fig. 4), and this characteristic would also be beneficial for DAF separation. From the *white-water* DAF performance eq. (SI Section S1), it is generally understood that increasing particle size can elevate DAF separation efficiency. This has been observed when particle sizes increased due to polymer-cell-organic matter bridging, thereby enhancing DAF separation efficiencies of several freshwater microalgal species [51,55,56]. Overall, these observations suggest that not all floc properties equally influence algal separation via sedimentation or DAF, and that the appropriate separation process can be selected based on the floc properties obtained.

4.2. Practical implications of using two flocculation methods and two separation processes for harvesting marine microalgal species

4.2.1. Between the flocculation methods

The practical implications of using both flocculation methods can be analysed from two standpoints – (a) chemical costs, and (b) downstream processing costs. With respect to chemical costs, dosing ferric chloride is cheaper than inducing alkaline flocculation. This is because the optimal dose of sodium hydroxide was approximately two orders of magnitude greater than that of ferric chloride (Fig. 1) while ferric chloride (~$230 per ton) was cheaper than sodium hydroxide (~$300 per ton). This suggests that the chemical costs of flocculating the marine microalgae *N. oculata* are ~$6 (ferric chloride flocculation) and ~ $200 (alkaline flocculation) per ton of biomass. The cost of alkaline flocculation can be further decreased by dosing other bases such as potassium, magnesium or calcium hydroxides [35,57]. Of these, calcium hydroxide (slaked

lime) was found to have the lowest dose requirement, cost per ton and handling risk [35]. At a slaked lime cost of $150 per ton, Vandamme et al. [35] estimated a chemical cost of $18 per ton of *Chlorella vulgaris* biomass harvested via alkaline flocculation. While the chemical costs during alkaline flocculation can be decreased, the success of alkaline flocculation is dependent on the presence of magnesium in the marine medium, and thus, it is important to replenish magnesium in subsequent cycles of culture medium reuse. Hence, these factors suggest that ferric chloride flocculation has cheaper chemical costs than alkaline flocculation.

Alkaline flocculation could be beneficial during downstream biomass processing, removal of the coagulant, and recuperation of the spent medium than dosing ferric chloride. Firstly, the high pH employed during alkaline flocculation is known to kill pathogenic microbes with negligible to minimal damage of the microalgal cells, thereby effectively sterilising the biomass and the culture medium [58]. Secondly, the switch from alkaline to neutral pH during the recuperation of the culture medium can be achieved by sparging the suspension with CO_2, which is more sustainable than chemical dosing [59]. Finally, ferric chloride is known to be toxic to the growth of microalgae e.g. *Auxenochlorella protothecoides* [60], which suggests that the coagulant removal from the harvested biomass is essential. However, the removal of ferric chloride is a challenging process often involving the application of EDTA or expensive electrochemical methods [61,62]. These reasons indicate that alkaline flocculation could be cheaper than ferric chloride flocculation when evaluating all the downstream costs.

4.2.2. Between the separation processes

The capital expenditure (CapEx) for the DAF process has been observed to be at least 3× greater than sedimentation while the operating expenditure (OpEx) for both processes were found to be largely similar [20]. This suggests that once the CapEx has been depreciated and amortised over time (~10 years), the harvesting costs for both processes would be comparable. Additionally, the DAF process results in a faster separation time of <10 min than sedimentation (~30 min). This would result in benefits such as a larger throughput of the harvested biomass over time and thus, a significantly lesser environmental footprint. Furthermore, the DAF process also produces a float layer with a solids content of ~3–5 % compared to sedimentation which produces a settled layer having a solids content of ~1.5 % [53]. Therefore, the dewatering costs of the harvested biomass would be cheaper in the case of DAF than sedimentation.

5. Conclusions

In this study, the floc property influences on the separation alkaline and ferric flocs of the seawater *Nannochloropsis oculata* via DAF and sedimentation were evaluated. Specific conclusions drawn from this work are as follows:

- Alkaline flocs were smaller, stronger and more compact than ferric flocs. The alkaline flocs also resisted breakage and underwent erosion into small (<10 μm) particles, whereas the low dose ferric flocs underwent breakage via fragmentation into larger (>100 μm) particles, and high dose ferric flocs underwent breakage via both fragmentation and erosion.
- As both, alkaline and ferric flocs were hydrophilic, sedimentation yielded ~15 % greater separation efficiency than the DAF process.
- Stoke's Law suggested that sedimentation benefited over DAF due to alkaline floc compactness and large sizes of ferric flocs.
- While not as effective as sedimentation, maximum separation efficiencies of ~80–85 % were obtained via DAF. For alkaline flocs, elevated bubble-floc attachment compensated for low hydrophilicity; for ferric flocs, low bubble-floc attachment was compensated by large floc sizes.
- The current study is the first of its kind to evaluate the physical properties of the flocs formed during alkaline flocculation and link them to separation outcomes via DAF and sedimentation. It is recommended that a kinetics assessment is undertaken in future studies in this line of research to provide mechanistic insights into the separation processes when applying alkaline flocculation.

CRediT authorship contribution statement

NRH Rao – Methodology, Visualisation, Formal analysis, Writing original draft, Data Curation.

A Gonzalez-Torres – Methodology, Review and editing.

B Tamburic – Review and editing.

YW Wong – Methodology.

K Muylaert – Review and editing.

I Foubert – Review and editing.

R Henderson – Conceptualisation, Methodology, Supervision, Resources, Review and editing.

D Vandamme – Conceptualisation, Methodology, Supervision, Formal analysis, Visualisation, Data curation, Review and editing, Funding Acquisition.

Declaration of competing interest

The authors declare the following financial interests/personal relationships which may be considered as potential competing interests:

Dries Vandamme reports financial support was provided by Research Foundation of Flanders, Belgium (FWO-12D8917N). Rita Henderson reports a relationship with Water Research Australia that includes: board membership. Rita Henderson reports editorial duties in the capacity of an Associate Editor for the journal Water Research.

Data availability

Data will be made available on request.

Acknowledgements

We would like to thank Ms. O. Vronska (Plant Functional Biology and Climate Change Cluster, UTS) for her assistance in culture setup and monitoring. We would also like to thank Mr. Camillo Taraborelli and Dr. Yun Ye for their technical support. DV was a post-doctoral researcher funded by the Research Foundation–Flanders, Belgium (FWO-12D8917N).

Appendix A. Supplementary data

Supplementary data to this article can be found online at https://doi.org/10.1016/j.algal.2023.103024.

References

[1] W. Mauser, G. Klepper, F. Zabel, R. Delzeit, T. Hank, B. Putzenlechner, A. Calzadilla, Global biomass production potentials exceed expected future demand without the need for cropland expansion, Nat. Commun. 6 (2015) 8946.
[2] N.R.H. Rao, B. Tamburic, Y.T.T. Doan, B.D. Nguyen, R.K. Henderson, Algal biotechnology in Australia and Vietnam: opportunities and challenges, Algal Res. 102335 (2021).
[3] C.A. Laamanen, G.M. Ross, J.A. Scott, Flotation harvesting of microalgae, Renew. Sust. Energ. Rev. 58 (2016) 75–86.
[4] D. Vandamme, I. Foubert, K. Muylaert, Flocculation as a low-cost method for harvesting microalgae for bulk biomass production, Trends Biotechnol. 31 (4) (2013) 233–239.
[5] A. Besson, P. Guiraud, High-pH-induced flocculation–flotation of the hypersaline microalga Dunaliella Salina, Bioresour. Technol. 147 (2013) 464–470.
[6] N. Fuad, R. Omar, S. Kamarudin, R. Harun, A. Idris, W.A. Wakg, Mass harvesting of marine microalgae using different techniques, Food and Bioproducts Processing 112 (2018) 169–184.

[7] G.P. Lam, M.H. Vermuë, G. Olivieri, L.A.M. van den Broek, M.J. Barbosa, M.H. M. Eppink, R.H. Wijffels, D.M.M. Kleinegris, Cationic polymers for successful flocculation of marine microalgae, Bioresour. Technol. 169 (2014) 804–807.
[8] S.O. Ajala, M.L. Alexander, Application of bio-based alkali to induce flocculation of microalgae biomass, Biomass Bioenergy 132 (2020), 105431.
[9] T. Chatsungnoen, Y. Chisti, Harvesting microalgae by flocculation–sedimentation, Algal Res. 13 (2016) 271–283.
[10] N.R.H. Rao, R.K. Henderson, 3rd Generation Biofuels, in: Elsevier, 2022, pp. 175–212.
[11] A. Schlesinger, D. Eisenstadt, A. Bar-Gil, H. Carmely, S. Einbinder, J. Gressel, Inexpensive non-toxic flocculation of microalgae contradicts theories; overcoming a major hurdle to bulk algal production, Biotechnol. Adv. 30 (5) (2012) 1023–1030.
[12] N.-A.T. Tran, J.R. Seymour, N. Siboni, C.R. Evenhuis, B. Tamburic, Photosynthetic carbon uptake induces autoflocculation of the marine microalga nannochloropsis oculata, Algal Res. 26 (2017) 302–311.
[13] N.-A.T. Tran, B. Tamburic, C.R. Evenhuis, J.R. Seymour, Bacteria-mediated aggregation of the marine phytoplankton Thalassiosira weissflogii and nannochloropsis oceanica, J. Appl. Phycol. 32 (6) (2020) 3735–3748.
[14] Q. Wang, K. Oshita, M. Takaoka, Flocculation properties of eight microalgae induced by aluminum chloride, chitosan, amphoteric polyacrylamide, and alkaline: life-cycle assessment for screening species and harvesting methods, Algal Res. 54 (2021), 102226.
[15] F.P. Camacho, V.S. Sousa, R. Bergamasco, M. Ribau Teixeira, The use of Moringa oleifera as a natural coagulant in surface water treatment, Chem. Eng. J. 313 (2017) 226–237.
[16] S. Walker, R.M. Narbaitz, Hollow fiber ultrafiltration of Ottawa River water: floatation versus sedimentation pre-treatment, Chem. Eng. J. 288 (2016) 228–237.
[17] N.A. Oladoja, G. Pan, Modification of local soil/sand with Moringa oleifera extracts for effective removal of cyanobacterial blooms, Sustain. Chem. Pharm. 2 (2015) 37–43.
[18] A. Pieterse, A. Cloot, Algal cells and coagulation, flocculation and sedimentation processes, Water Sci. Technol. 36 (4) (1997) 111–118.
[19] A. Besson, C. Formosa-Dague, P. Guiraud, Flocculation-flotation harvesting mechanism of Dunaliella salina: from nanoscale interpretation to industrial optimization, Water Res. 155 (2019) 352–361.
[20] N. Deconinck, K. Muylaert, W. Ivens, D. Vandamme, Innovative harvesting processes for microalgae biomass production: a perspective from patent literature, Algal Res. 31 (2018) 469–477.
[21] V.R. Fanaie, M. Khiadani, Effect of salinity on air dissolution, size distribution of microbubbles, and hydrodynamics of a dissolved air flotation (DAF) system, Colloids Surf. A Physicochem. Eng. Asp. 591 (2020), 124547.
[22] J. Haarhoff, J.K. Edzwald, Adapting dissolved air flotation for the clarification of seawater, Desalination 311 (2013) 90–94.
[23] Y. Shutova, B.L. Karna, A.C. Hambly, B. Lau, R.K. Henderson, P. Le-Clech, Enhancing organic matter removal in desalination pretreatment systems by application of dissolved air flotation, Desalination 383 (2016) 12–21.
[24] J.K. Edzwald, Dissolved air flotation and me, Water Res. 44 (7) (2010) 2077–2106.
[25] J. Haarhoff, J.K. Edzwald, Dissolved air flotation modelling: insights and shortcomings, J. Water Supply Res Technol. 53 (3) (2004) 127–150.
[26] S. Garg, Y. Li, L. Wang, P.M. Schenk, Flotation of marine microalgae: effect of algal hydrophobicity, Bioresour. Technol. 121 (2012) 471–474.
[27] A. Gonzalez-Torres, M. Pivokonsky, R. Henderson, The impact of cell morphology and algal organic matter on algal floc properties, Water Res. 163 (2019), 114887.
[28] G.P. Lam, J.B. Giraldo, M.H. Vermuë, G. Olivieri, M.H.M. Eppink, R.H. Wijffels, Understanding the salinity effect on cationic polymers in inducing flocculation of the microalga neochloris oleoabundans, J. Biotechnol. 225 (2016) 10–17.
[29] S. Lama, K. Muylaert, T.B. Karki, I. Foubert, R.K. Henderson, D. Vandamme, Flocculation properties of several microalgae and a cyanobacterium species during ferric chloride, chitosan and alkaline flocculation, Bioresour. Technol. 220 (2016) 464–470.
[30] L. Li, G. Pan, A universal method for flocculating harmful algal blooms in marine and fresh waters using modified sand, Environ. Sci. Technol. 47 (9) (2013) 4555–4562.
[31] N. Uduman, Y. Qi, M.K. Danquah, A.F.A. Hoadley, Marine microalgae flocculation and focused beam reflectance measurement, Chem. Eng. J. 162 (3) (2010) 935–940.
[32] J.K. Edzwald, Principles and applications of dissolved air flotation, Water Sci. Technol. 31 (3–4) (1995) 1–23.
[33] A. Gonzalez-Torres, J. Putnam, B. Jefferson, R.M. Stuetz, R.K. Henderson, Examination of the physical properties of Microcystis aeruginosa flocs produced on coagulation with metal salts, Water Res. 60 (2014) 197–209.
[34] A. Gonzalez-Torres, A.M. Rich, C.E. Marjo, R.K. Henderson, Evaluation of biochemical algal floc properties using Reflectance Fourier-Transform Infrared Imaging, Algal Research 27 (2017) 345–355.
[35] D. Vandamme, I. Foubert, I. Fraeye, B. Meesschaert, K. Muylaert, Flocculation of Chlorella vulgaris induced by high pH: role of magnesium and calcium and practical implications, Bioresour. Technol. 105 (2012) 114–119.
[36] J. Duan, J. Gregory, Coagulation by hydrolysing metal salts, Adv. Colloid Interface Sci. 100 (2003) 475–502.
[37] D. Vandamme, K. Muylaert, I. Fraeye, I. Foubert, Floc characteristics of Chlorella vulgaris: influence of flocculation mode and presence of organic matter, Bioresour. Technol. 151 (2014) 383–387.
[38] Z. Mustafa, N. Rao, R. Henderson, G. Leslie, P. Le-Clech, Considerations of the limitations of commonly applied characterisation methods in understanding protein-driven irreversible fouling, Environ. Sci.: Water Res. Technol. 8 (2) (2022) 343–357.
[39] N. Subhi, A.R.D. Verliefde, V. Chen, P. Le-Clech, Assessment of physicochemical interactions in hollow fibre ultrafiltration membrane by contact angle analysis, J. Membr. Sci. 403–404 (2012) 32–40.
[40] P. Jarvis, B. Jefferson, J. Gregory, S.A. Parsons, A review of floc strength and breakage, Water Res. 39 (14) (2005) 3121–3137.
[41] Z. Yang, J. Hou, L. Miao, Harvesting freshwater microalgae with natural polymer flocculants, Algal Res. 57 (2021), 102358.
[42] R.K. Henderson, S.A. Parsons, B. Jefferson, Surfactants as bubble surface modifiers in the flotation of algae: dissolved air flotation that utilizes a chemically modified bubble surface, Environ. Sci. Technol. 42 (13) (2008) 4883–4888.
[43] G.S. Aléman-Nava, K. Muylaert, S.P.C. Bermudez, O. Depraetere, B. Rittmann, R. Parra-Saldívar, D. Vandamme, Two-stage cultivation of Nannochloropsis oculata for lipid production using reversible alkaline flocculation, Bioresour. Technol. 226 (2017) 18–23.
[44] P. Palaniandy, M.N. Adlan, H.A. Aziz, M.F. Murshed, Y.-T. Hung, Handbook of Advanced Industrial and hazardous Wastes Management, in: CRC Press, 2017, pp. 657–694.
[45] H. Sun, R. Jiao, H. Xu, G. An, D. Wang, The influence of particle size and concentration combined with pH on coagulation mechanisms, J. Environ. Sci. 82 (2019) 39–46.
[46] L. Pérez, J.L. Salgueiro, R. Maceiras, Á. Cancela, Á. Sánchez, Study of influence of pH and salinity on combined flocculation of Chaetoceros gracilis microalgae, Chem. Eng. J. 286 (2016) 106–113.
[47] A. Suresh, E. Grygolowicz-Pawlak, S. Pathak, L.S. Poh, D. Dominiak, T.V. Bugge, X. Gao, W.J. Ng, M. bin Abdul Majid, Understanding and optimization of the flocculation process in biological wastewater treatment processes: A review, Chemosphere 210 (2018) 401–416.
[48] C. Formosa-Dague, V. Gernigon, M. Castelain, F. Daboussi, P. Guiraud, Towards a better understanding of the flocculation/flotation mechanism of the marine microalgae Phaeodactylum tricornutum under increased pH using atomic force microscopy, Algal Res. 33 (2018) 369–378.
[49] L. Chekli, E. Corjon, S.A.A. Tabatabai, G. Naidu, B. Tamburic, S.H. Park, H.K. Shon, Performance of titanium salts compared to conventional FeCl3 for the removal of algal organic matter (AOM) in synthetic seawater: coagulation performance, organic fraction removal and floc characteristics, J. Environ. Manag. 201 (2017) 28–36.
[50] L. Chekli, C. Eripret, S. Park, S.A.A. Tabatabai, O. Vronska, B. Tamburic, J. Kim, H. Shon, Coagulation performance and floc characteristics of polytitanium tetrachloride (PTC) compared with titanium tetrachloride (TiCl4) and ferric chloride (FeCl3) in algal turbid water, Sep. Purif. Technol. 175 (2017) 99–106.
[51] R.K. Henderson, S.A. Parsons, B. Jefferson, Polymers as bubble surface modifiers in the flotation of algae, Environ. Technol. 31 (7) (2010) 781–790.
[52] M. Zhang, X. Lu, Q. Zhou, L. Xie, C. Shen, Polyaluminum chloride-functionalized colloidal gas aphrons for flotation separation of nanoparticles from water, J. Hazard. Mater. 362 (2019) 196–205.
[53] J.C. Crittenden, R.R. Trussell, D.W. Hand, K.J. Howe, G. Tchobanoglous, MWH's Water Treatment: Principles and Design, John Wiley & Sons, 2012.
[54] H. Zhang, L. Yang, X. Zang, S. Cheng, X. Zhang, Effect of shear rate on floc characteristics and concentration factors for the harvesting of Chlorella vulgaris using coagulation-flocculation-sedimentation, Sci. Total Environ. 688 (2019) 811–817.
[55] N.R.H. Rao, R. Yap, M. Whittaker, R.M. Stuetz, B. Jefferson, W.L. Peirson, A. M. Granville, R.K. Henderson, The role of algal organic matter in the separation of algae and cyanobacteria using the novel "Posi" - dissolved air flotation process, Water Res. 130 (2018) 20–30.
[56] L. Yang, H. Zhang, S. Cheng, W. Zhang, X. Zhang, Enhanced microalgal harvesting using microalgae-derived extracellular polymeric substance as flocculation aid, ACS Sustain. Chem. Eng. 8 (10) (2020) 4069–4075.
[57] H.P. Vu, L.N. Nguyen, M.T. Vu, L. Labeeuw, B. Emmerton, A.S. Commault, P. J. Ralph, T. Mahlia, L.D. Nghiem, Harvesting Porphyridium purpureum using polyacrylamide polymers and alkaline bases and their impact on biomass quality, Sci. Total Environ. 755 (2021), 142412.
[58] D. Kaloudas, N. Pavlova, R. Penchovsky, Phycoremediation of wastewater by microalgae: a review, Environ. Chem. Lett. 19 (4) (2021) 2905–2920.
[59] S. Ge, P. Champagne, H. Wang, P.G. Jessop, M.F. Cunningham, Microalgae recovery from water for biofuel production using CO2-switchable crystalline nanocellulose, Environ. Sci. Technol. 50 (14) (2016) 7896–7903.
[60] E. Polat, E. Yüksel, M. Altınbaş, Effect of different iron sources on sustainable microalgae-based biodiesel production using auxenochlorella protothecoides, Renew. Energy 162 (2020) 1970–1978.
[61] E.M. Likosova, J. Keller, Y. Poussade, S. Freguia, A novel electrochemical process for the recovery and recycling of ferric chloride from precipitation sludge, Water Res. 51 (2014) 96–103.
[62] E.K. Tetteh, S. Rathilal, Application of organic coagulants in water and wastewater treatment, Org. Polym. 1 (2019) 51–68.